computers

MDPI

Article

A Computational Algorithm for Optimal Resource Allocation in Nonlinear Multi-Module Systems with Bilateral Constraints

Kamshat Tussupova *, Gulbanu Mirzakhmedova, Diana Rakhimova and Zhansaya Duisenbekkyzy

Department of Information Systems, Al-Farabi Kazakh National University, Al-Farabi Ave. 71/23, Almaty 050040, Kazakhstan; gulbanu.mirzakhmedova@kaznu.edu.kz (G.M.); diana.rakhimova@kaznu.edu.kz (D.R.); duisenbekkyzy.zh@kaznu.kz (Z.D.)
* Correspondence: kamshat.tusupova@kaznu.edu.kz; Tel.: +7-702-466-22-65

Abstract

This study addresses the problem of optimal resource allocation in nonlinear multi-module dynamic systems arising in complex computational and techno-economic processes, where numerical stability and strict enforcement of structural constraints are critical. The objective is to develop a computationally efficient optimal control algorithm capable of handling bilateral control constraints and external balance conditions without resorting to large-scale nonlinear programming or boundary-value shooting. The proposed method is based on a modified Lagrangian formulation, in which bilateral Karush–Kuhn–Tucker (KKT) conditions are analytically embedded into the optimality system. The resulting computational scheme consists of a coupled system of matrix and vector differential equations solved through a non-iterative backward–forward integration procedure. Numerical experiments conducted on a nonlinear model with Cobb–Douglas-type operators demonstrate the stable convergence of the trajectories toward a stationary regime, strict satisfaction of bilateral constraints, and consistent enforcement of balance relations throughout the planning horizon. Empirical scalability analysis indicates approximately cubic computational complexity with respect to the state dimension, while sensitivity tests confirm the numerical robustness across different integration tolerances and ODE solvers. These results demonstrate that the proposed structure-preserving framework provides a computationally stable and practically implementable approach to constrained optimal control in nonlinear multi-module systems.

Keywords: computational optimal control; numerical algorithms; nonlinear dynamic systems; constrained optimization; resource allocation; Riccati-based methods; multi-module systems

Academic Editor: Paolo Bellavista

Received: 30 January 2026
Revised: 4 March 2026
Accepted: 6 March 2026
Published: 9 March 2026

1. Introduction

The development of numerically stable and computationally efficient optimal control algorithms for nonlinear dynamic systems with constraints remains one of the key unresolved challenges in modern computational science. In practical implementations of such algorithms, the main difficulty lies not in the formulation of optimality conditions but in ensuring the accurate enforcement of resource and balance constraints at every computational step without the loss of stability and convergence. This problem becomes particularly acute in control tasks involving complex systems with a large number of interacting subsystems [1–3], characterized by complex interactions between subsystems, the presence of feedback loops, and the redistribution of limited resources. Such structures arise in the modeling of distributed computing systems [4], production and logistics networks, energy and telecommunication complexes, and in control problems of large socio-economic and technogenic systems [3,5]. In such problems, the presence of state-dependent input operators [6] and bilateral control constraints [7,8] significantly complicates both the analytical treatment and the numerical synthesis of control.

Optimal control problems for multi-module nonlinear systems are formulated as problems of resource redistribution among modules subject to dynamic, structural, and balance conditions. In such formulations, control actions are typically vector-valued and influence the system through nonlinear operators depending on the current state. The presence of bilateral control constraints, which are typical for practical applications, leads to nonsmooth control laws and significantly complicates the application of standard optimal control methods. If the model additionally includes differential–algebraic (DAE) relations, the preservation of algebraic consistency during numerical integration becomes critical and requires structure-preserving computational schemes.

For DAE systems, standard numerical integration and optimization methods [9,10] are inapplicable without substantial modifications, since strict consistency between the differential and algebraic parts of the model must be maintained at each computational step [11]. Violation of this consistency leads to the accumulation of numerical errors and the loss of the physical interpretability of solutions, making the development of specialized computational schemes a fundamentally important task.

Numerical optimal control methods for nonlinear constrained systems are traditionally divided into indirect and direct approaches. Indirect methods, based on the Pontryagin maximum principle, provide the necessary optimal conditions but lead to two-point boundary-value problems [2,12,13] that are sensitive to the initialization of adjoint variables and often require iterative shooting procedures [14]. Forward–backward sweep techniques extend this paradigm to constrained nonlinear systems; however, they typically retain sensitivity to boundary conditions and may require iterative refinement [15].

Direct methods, including transcription and collocation schemes, discretize the state and control trajectories and reformulate the optimal control problem as a nonlinear programming (NLP) problem [16,17]. Modern implementations such as GPOPS-II rely on hp-adaptive collocation and large-scale NLP solvers to handle complex constraints [18]. While highly flexible, these approaches require iterative optimization and do not directly yield analytic feedback structures.

Model Predictive Control (MPC), particularly in its nonlinear form, addresses constrained control through repeated finite-horizon optimization [19]. Although effective in practice, nonlinear MPC remains computationally demanding for high-dimensional systems due to the necessity of solving an optimization problem at each sampling instant.

In parallel, reinforcement learning (RL) has emerged as a data-driven framework for approximating optimal control policies [20] in continuous control problems. Recent studies emphasize conceptual connections between RL and classical optimal control, including links to Riccati theory in linear–quadratic settings [21]. However, RL-based approaches typically rely on training procedures and do not inherently preserve the structural balance constraints during continuous-time integration.

Operator-learning frameworks, including neural operator architectures, approximate solution operators of differential equations using data-driven mappings [22]. These methods provide powerful surrogate models for complex dynamics but are primarily oriented toward system approximation rather than variationally derived feedback synthesis with explicitly embedded control constraints.

The proposed framework establishes a variational formulation that analytical embedding of bilateral KKT conditions into the optimality system of nonlinear dynamic models whose controlled structure exhibits bilinear state–input coupling. This construction leads to a closed system of coupled matrix and vector differential equations that can be solved within a non-iterative two-pass integration scheme. By determining the initial value of the adjoint variable analytically through the transition matrix representation, the proposed method avoids the iterative boundary-value shooting procedures typically associated with indirect approaches. At the same time, the resulting computational structure preserves the variational nature of the optimality conditions and demonstrates numerical feasibility and stability for the considered class of constrained multi-module systems.

2. Materials and Methods

2.1. Nonlinear Multi-Module Dynamic Model

Consider a computational model of a nonlinear multi-module dynamic system consisting of three interacting functional modules: $i = 0$—production module, $i = 1$—investment module, $i = 2$—consumer module. Each module processes resources and generates output according to a parametric production operator represented by a Cobb–Douglas-type function:

$$X_i = F_i(K_i,\ L_i) = A_i K_i^{\alpha_i} L_i^{1-\alpha_i},\ \ (i = 0,\ 1,\ 2), \tag{1}$$

where X_i is the output generated by module i, K_i and L_i denote the capital and labor assigned to module i, A_i is the coefficient of neutral technological progress, α_i is the capital elasticity coefficient, and $(1 - \alpha_i)$ is the labor elasticity coefficient [5,23].

To express the system in a compact computation-oriented form, we introduce normalized and structural variables widely used in dynamic system modeling:

$\theta_i = \frac{L_i}{L}$: shares in labor resource distribution across modules.
$s_i = \frac{I_i}{X_1}$: shares in investment resource distribution across modules.
$f_i(k_i) = \frac{X_i}{L_i}$: labor productivity in the i-th module.
$k_i = \frac{K_i}{L_i}$: capital–labor ratio of the modules.
$\sigma_1 = \frac{Y_1}{L}$: external inflow ratio for investment.
$\sigma_2 = \frac{Y_2}{L}$: external inflow ratio for consumption.
$x_i = \theta_i f_i(k_i)$: normalized output of module i.

Using these structural variables, the operator (1) can be rewritten in a capital–labor intensity form, which is more convenient for computational analysis:

$$\dot{k}_i(t) = -\tau_i k_i(t) + \frac{s_i}{\theta_i}(x_1 + \sigma_1),\ \ k_i(0) = k_i^0,\ \ \tau_i > 0, \tag{2}$$

$$x_i = \theta_i A_i k_i^{\alpha_i},\ \ A_i > 0,\ \ 0 < \alpha_i < 1,\ \ i = 0,\ 1,\ 2. \tag{3}$$

The system dynamics are further constrained by several resource-flow and external-exchange relations, which ensure the consistency of the multi-module system:

Investment balance:

$$s_0 + s_1 + s_2 = 1,\ \ s_i > 0,\ \ i = 0,\ 1,\ 2. \tag{4}$$

Labor balance:

$$\theta_0 + \theta_1 + \theta_2 = 1,\ \ \theta_i > 0,\ \ i = 0,\ 1,\ 2. \tag{5}$$

Material balance:

$$(1 - \beta_0)x_0 = \beta_1 x_1 + \beta_2 x_2 + \sigma_0,\ \ 0 < \beta_i < 1,\ \ \ i = 0,\ 1,\ 2. \tag{6}$$

Foreign trade balance:

$$h_0\sigma_0 = h_1\sigma_1 + h_2\sigma_2. \tag{7}$$

Industrial security:

$$\sigma_1 \leq \gamma_1 x_1, \quad \sigma_2 \leq \gamma_2 x_2. \tag{8}$$

Here, $\gamma_1,\ \gamma_2$ represent import quota coefficients for investment and consumer goods, σ_0 is the export share for material flows, and $\sigma_1,\ \sigma_2$ are the volumes of imports of investment and consumer goods, respectively; h_0 is the world price of exported materials, $h_1,\ h_2$ are the world prices of imported investment and consumer goods, τ_i describes the capital depreciation and labor-growth effects, and β_i represents the direct material costs per unit of output in the i-th module.

In the optimal configuration, the import volumes are determined by their admissible upper bounds specified in (8), which gives

$$\sigma_1 = \gamma_1 x_1, \quad \sigma_2 = \gamma_2 x_2. \tag{9}$$

Substituting (9) into the capital–labor intensity Equation (2), and using representation (3), the dynamic Equation (2) takes the following form:

$$\dot{k}_i(t) = -\tau_i k_i(t) + \frac{s_i}{\theta_i}(1+\gamma_1)\theta_1 A_1 k_1{}^{\alpha_1},\ k_i(0) = k_i^0,\ \ \lambda_i > 0, \tag{10}$$

A numerical method for determining a stable system configuration, based on the Lagrange multiplier driven optimization scheme combined with the golden-section search principle, was originally proposed in [5].

2.2. Computational Formulation of the Control Problem

In this study, the condition of stable system functioning is formalized through structural constraints that preserve admissible equilibrium trajectories and enforce consistency between resource flows and control variables.

Since the system (2)–(8) contains six control variables, it can be reduced to a system with three controls by applying the resource-flow balance relations. To simplify the notation, we introduce the following state variables:

$$y_0(t) = k_0(t),\ \ y_1(t) = k_1(t),\ \ y_2(t) = k_2(t), \tag{11}$$

and we define the corresponding control variables as

$$u_0(t) = \frac{s_0\theta_1}{\theta_0},\ \ u_1(t) = s_1,\ \ u_2(t) = \frac{s_2\theta_1}{\theta_2}. \tag{12}$$

As a result of the transformations performed, system (10) takes the following form:

$$\dot{y}_i(t) = -\tau_i y_i(t) + (1+\gamma_1)A_1 u_i(t) y_1(t)^{\ \alpha_1},\ \ y_i(t_0) = y_i^0,\ \ y_i(T) = 0,\ i = 0,1,2. \tag{13}$$

Next, we rewrite system (13) in vector–matrix form and consider the controlled nonlinear dynamical system of the following form:

$$\dot{y}(t) = Ay(t) + BD(y)u(t),\ \ y(t_0) = y_0,\ \ y(T) = 0, \tag{14}$$

subject to the following control constraints:

$$u(t) \in U(t) = \{u | \rho_1(t) \leq u(t) \leq \rho_2(t), t \in [t_0, T]; \rho_1, \rho_2 \in C[t_0, T]\} \tag{15}$$

where $y(t) \in \mathbb{R}^n$ is the state vector, and $u(t) \in \mathbb{R}^m$ is the control vector.

The system matrices are given by

$$A = \begin{pmatrix} -\tau_0 & 0 & 0 \\ 0 & -\tau_1 & 0 \\ 0 & 0 & -\tau_2 \end{pmatrix}, \; B = \begin{pmatrix} (1+\gamma_1)A_1 & 0 & 0 \\ 0 & (1+\gamma_1)A_1 & 0 \\ 0 & 0 & (1+\gamma_1)A_1 \end{pmatrix}, D(y) = \begin{pmatrix} y_1(t)^{\alpha_1} & 0 & 0 \\ 0 & y_1(t)^{\alpha_1} & 0 \\ 0 & 0 & y_1(t)^{\alpha_1} \end{pmatrix}.$$

The matrices $A(t) \in \mathbb{R}^{n \times n}$ and $B(t) \in \mathbb{R}^{n \times m}$ are given and describe the internal structure of the system as well as the influence of the control inputs on its dynamics. The matrix $D(y) \in \mathbb{R}^{m \times m}$ is a diagonal matrix that defines the nonlinear dependence of the control on the system state. The initial and terminal times are denoted by t_0 and T, respectively. It is assumed that system (14) is controllable at time t_0.

The objective of control is to minimize the performance functional, which measures deviations of the state and control from their stationary values (y_s, u_s):

$$\begin{aligned} J(y,u) = \; & \tfrac{1}{2}\int_{t_0}^{T}\left[(y(t)-y_s)^T Q(y(t)-y_s) + (D(y)u(t) - D_s u_s)^T R(D(y)u(t) - D_s u_s)\right]dt \\ & + \tfrac{1}{2}(y(T)-y_s)^T F(y(T)-y_s) \end{aligned} \tag{16}$$

$Q(t) \in \mathbb{R}^{n \times n}$ is a symmetric nonnegative-definite weight matrix penalizing deviations of the system state from equilibrium, $R(t) \in \mathbb{R}^{m \times m}$ is a symmetric positive-definite matrix reflecting the cost of resource reallocation, and F is the terminal penalty matrix.

The problem is to construct a control function $u(t)$ that transfers system (14) from the initial state $y(t_0) = y_0$ to the desired terminal state $y(T) = 0$, while satisfying the bilateral constraints (15) and minimizing the performance functional (16).

2.3. *Computational Construction of the Feedback Law*

To solve the problem, we apply a modified Lagrangian formulation. The main idea of this method is to transform the original constrained problem into an equivalent unconstrained problem, the solution of which automatically satisfies the initial constraints.

To construct the computational scheme, we introduce the auxiliary function

$$v(y,t) = \frac{1}{2}(y(t)-y_s)^T K (y(t)-y_s) + q(t)^T (y(t)-y_s), \tag{17}$$

where $K \in \mathbb{R}^{n \times n}$ is a time-varying matrix, and $q(t) \in \mathbb{R}^n$ is a time-dependent vector.

The choice of this quadratic structure is dictated by the intrinsic properties of the performance functional, which is quadratic with respect to the deviations of the state and control variables from their stationary values. A quadratic form represents the simplest function capable of adequately capturing the local dependence of the optimal cost on the state deviation.

The adjoint variable is defined as the gradient of the auxiliary function with respect to the state:

$$\lambda_0(y,t) = \frac{\partial v(y,t)}{\partial y} = K(y(t)-y_s) + q(t). \tag{18}$$

Thus, the adjoint variable becomes linear in the state, which is essential for reducing the optimality system to a matrix differential equation for $K(t)$.

Since the matrix K and the vector $q(t)$ depend explicitly on time, the partial derivative of $v(y,t)$ with respect to time is given by

$$\frac{\partial v(y,t)}{\partial t} = \frac{1}{2}(y(t)-y_s)^T \dot{K} (y(t)-y_s) + (y(t)-y_s)^T \dot{q}(t). \tag{19}$$

The multipliers $\lambda_1(y,t)$ and $\lambda_2(y,t)$ are introduced to enforce the bilateral control constraints (17). According to the KKT framework, these constraints are written as

$$\rho_1 - u(t) \leq 0, \;\; u(t) - \rho_2 \leq 0.$$

According to the KKT framework, these constraints are incorporated using nonnegative multipliers, satisfying the following complementarity conditions:

$$\lambda_1^T(y,t)(\rho_1 - u(t)) = 0, \;\; \lambda_2^T(y,t)(u(t) - \rho_2) = 0, \;\; \lambda_i(y,t) \geq 0, \;\; (i = 1,\, 2).$$

To preserve consistency with the quadratic control weighting in the performance functional, the constraints are introduced in the weighted form involving $D^T(y)RD(y)$.

To ensure consistency between the state deviation and its linear representation through the transition matrix $W(t,T)$, an additional Lagrange multiplier $\lambda_3(y,t)$ is introduced. This multiplier makes it possible to incorporate into the variational formulation of the following relation:

$$y(t) - y_s = W(t,T)\, q(t), \;\; t \in [t_0, T] \tag{20}$$

where $W(t,T)$ is a transition matrix, which follows from the linear structure of the obtained adjoint equation.

In the extended Lagrangian functional, the corresponding term is written in the following form:

$$\lambda_3^T(y,t)(y(t) - y_s - W(t,T)q(t)).$$

Combining the performance functional, system dynamics, and constraint terms, we obtain the modified Lagrangian functional as

$$\begin{aligned} L(y,u) = J(y,u) \quad & + \int_{t_0}^{T} \big((K(y(t) - y_s) + q(t))^T (A(y(t) - y_s) + B(D(y)u(t) - D_s u_s) \\ & - \dot{y}(t)) + \lambda_1^T(y,t) D^T(y) R D(y(t))(\rho_1 - u(t)) \\ & + \lambda_2^T(y,t) D^T(y) R D(y)(u(t) - \rho_2) \\ & + \lambda_3^T(y,t)\, (y(t) - y_s - W(t,T)q(t))\big) dt. \end{aligned} \tag{21}$$

2.4. Riccati-Based Feedback Synthesis for Bilinear Constrained Systems

2.4.1. Reformulation of the Extended Lagrangian

Using the identity for the total time derivative of the auxiliary function

$$\frac{dv(y,t)}{dt} = \frac{\partial v}{\partial y}^T \dot{y}(t) + \frac{\partial v}{\partial t}, \tag{22}$$

and taking into account that $\lambda_0(y,t) = \frac{\partial v}{\partial y}$, the term $\lambda_0^T(y,t)(-\dot{y}(t))$ in the extended Lagrangian can be rewritten as a total derivative plus a time-variation term.

After integration over $[t_0, T]$, the total derivative generates the boundary contributions $v(y_0, t_0) - v(y(T), T)$, while the remaining integral depends only on the state, control, and multipliers.

Collecting these terms together with the performance functional and the constraint contributions leads to a reduced integrand representation of the extended Lagrangian.

For the convenience of further analysis, we introduce the auxiliary integrand $M(y,u)$, which gathers all terms depending on the state, control variables, and multipliers:

$$\begin{aligned} M(y,u) = \ & \tfrac{1}{2}(y(t)-y_s)^T\Big[Q+\dot{K}\Big](y(t)-y_s)+\tfrac{1}{2}(D(y)u(t)-D_s u_s)^T R(D(y)u(t) \\ & -D_s u_s)+(K(y(t)-y_s) \\ & +q(t))^T(A(y(t)-y_s)+B(D(y)u(t)-D_s u_s))+(y(t)-y_s)\dot{q}(t) \\ & +\lambda_1^T(y,t)D^T(y)RD(y)(\rho_1-u(t))+\lambda_2^T(y,t)D^T(y)RD(y)(u(t)-\rho_2) \\ & +\lambda_3^T(y,t)(y(t)-y_s-W(t,T)q(t)). \end{aligned} \quad (23)$$

Substituting the expression for $M(y,u)$ into the functional (21), we obtain an extended form of the Lagrangian functional as

$$L(y,u)=v(y_0,t_0)-v(y(T),T)+\int_{t_0}^{T} M(y,u)dt+\frac{1}{2}(y(T)-y_s)^T F(y(T)-y_s). \quad (24)$$

2.4.2. First-Order Optimality Condition with Respect to the Control

To determine the computed trajectories, we apply the first-order necessary optimality conditions, which are obtained by setting to zero the partial derivatives of the function $M(y,u)$ (24) with respect to the control variables $u(t)$:

$$\begin{aligned} \tfrac{\partial M(y,u)}{\partial u(t)} &= D(y)u(t)-D_s u_s+B^T R^{-1}(K(y(t)-y_s)+q(t)) \\ & \quad -D(y)(\lambda_1(y,t)-\lambda_2(y,t))=0 \end{aligned} \quad (25)$$

As a result, we obtain the following relation:

$$D(y)u(t)-D_s u_s=-R^{-1}B^T(K(y(t)-y_s)+q(t))+D(y)(\lambda_1(y,t)-\lambda_2(y,t)), \quad (26)$$

from which, by solving for $u(t)$, we derive an explicit representation of the computed control:

$$u(t)=D(y)^{-1}\Big(D_s u_s-R^{-1}B^T(K(y(t)-y_s)+q(t))\Big)+\lambda_1(y,t)-\lambda_2(y,t). \quad (27)$$

2.4.3. First-Order Optimality Condition with Respect to the State

$$\begin{aligned} \tfrac{\partial M(y,u)}{\partial y(t)} = \ & \Big(Q+\dot{K}\Big)(y(t)-y_s)+K(A(y(t)-y_s)+B(D(y)u(t)-D_s u_s)) \\ & +A^*(K(y(t)-y_s)+q(t))+\dot{q}(t)+\lambda_3^T(y,t)=0 \end{aligned} \quad (28)$$

Substituting expression (27) into (28) and grouping terms with respect to the state deviation, we obtain an equation that links the state vector and the adjoint variables, as follows:

$$\begin{aligned} & \Big(Q+\dot{K}+KA+A^T K-KBR^{-1}B^T K\Big)(y(t)-y_s)-KBR^{-1}B^T q(t) \\ & +KBD(y)(\lambda_1(y,t)-\lambda_2(y,t))+A^T q(t)+\dot{q}(t)+\lambda_3^T(y,t)=0 \end{aligned} \quad (29)$$

2.4.4. Riccati-Type Matrix Equation for K

Consider the part of expression (29) that is quadratic with respect to the state deviation. To ensure the consistency of the optimality conditions, the coefficient multiplying $(y(t)-y_s)$ must vanish. This requirement leads to the following matrix differential equation:

$$\dot{K}+KA+A^T K-KBR^{-1}B^T K+Q(t)=0, \quad K(T)=F \quad (30)$$

https://doi.org/10.3390/computers15030179

The obtained relation represents a matrix differential equation of the Riccati type and determines the evolution of the matrix K.

2.4.5. Derivation of the Linear Adjoint Equation

After eliminating the quadratic term from (29), we obtain the following linear equation for $q(t)$:

$$\dot{q}(t) = -(A - KB_1)q(t) - KBD(y)(\lambda_1(y,t) - \lambda_2(y,t)) - \lambda_3^T(y,t). \quad (31)$$

To obtain a differential equation for $q(t)$, the multiplier $\lambda_3(y,t)$ is selected to preserve equivalence between the augmented variational formulation and the original constrained optimal control problem by enforcing compatibility between the state–adjoint representation and the transition mapping. This construction guarantees that no additional optimality conditions beyond the original problem are introduced:

$$\lambda_3^T(y,t) = -\left(K - W^{-1}(t,T)\right)BD(y)(\lambda_1(y,t) - \lambda_2(y,t)). \quad (32)$$

Substituting this expression into Equation (31) results in cancelation and yields the final form equation for $q(t)$:

$$\dot{q}(t) = -A_1 q(t) + W^{-1}(t,T)BD(y)(\lambda_1(y,t) - \lambda_2(y,t)), \ \ q(T) = (F - K(T))(y(T) - y_s), \quad (33)$$

where

$$A_1 = A - BR^{-1}B^T K. \quad (34)$$

Thus, the multiplier $\lambda_3(y,t)$ is not introduced arbitrarily but is determined by the requirement of consistency of the linear state representation and the differential equation for $q(t)$.

2.4.6. Consistency Condition and Transition Matrix Equation

To ensure the dynamic consistency of the representation (20), we differentiate it with respect to time, which yields

$$\dot{y}(t) = \dot{W}(t,T)q(t) + W(t,T)\dot{q}(t). \quad (35)$$

Substituting the expression for $\dot{q}(t)$ and the state equation with the computed control law into (35) and equating the coefficients of $q(t)$ on both sides, we obtain the differential equation governing the transition matrix, as follows:

$$\dot{W}(t,T) = W(t,T){A_1}^T(t) + A_1(t)W(t,T) - BR^{-1}B^T, \ W(T,T) = \left(F - K(T)\right)^{-1}. \quad (36)$$

The terminal condition follows from the definition of $q(T)$.

2.4.7. Feedback Law Under Bilateral Constraints

We introduce the following notation:

$$\varphi(y,t) = \lambda_1(y,t) - \lambda_2(y,t), \quad (37)$$

where

$$\lambda_1(y,\ t) = max\ \{0;\ \gamma_1 - \omega(y,t)\} \geq 0,\ \ \lambda_2(y,\ t) = max\ \{0;\ \omega(y,t) - \gamma_2\} \geq 0, \quad (38)$$

$$\omega(y,\ t) = D^{-1}(y)\left(D_s u_s - R^{-1}B^T(K(y(t) - y_s) + q(t))\right). \quad (39)$$

The resulting optimal state trajectory in feedback form is given by

$$\dot{y}(t) = A_1 y(t) - BR^{-1}B^T q(t) + BD(y)\varphi(y,t), \;\; y(t_0) = y_0. \tag{40}$$

The joint solution of the system of equations for K, $q(t)$, and $W(t,T)$ enforces structural consistency under the assumed regularity conditions between the dynamics of the state, the adjoint variables, and the terminal condition.

We formulate the obtained results in the form of the following theorem.

Theorem 1. *Assume that, on the interval $t_0 \leq t \leq T$, the matrix Q is symmetric and positive semidefinite, while the matrices R, F, and $D(y)$ are symmetric and positive definite. Furthermore, assume that the matrix $W(t_0, T)$ is positive definite and that system (14) is controllable at time t_0. Under these conditions, the proposed algorithm generates a defined feedback trajectory satisfying the following necessary optimality conditions:*

$$\dot{y}(t) = A_1 y(t) - BR^{-1}B^T q(t) + BD(y)\varphi(y,t), \;\; y(t_0) = y_0,$$

while the optimal control is given by

$$u(t) = \omega(y,t) + \varphi(y,t),$$

in which $\lambda_1(y,t)$ and $\lambda_2(y,t)$ are the Lagrange multipliers ensuring the satisfaction of the bilateral control constraints:

$$\rho_1(t) \leq u(t) \leq \rho_2(t).$$

2.4.8. Computational Enforcement of Resource Constraints

To verify compliance with the balance constraints, the following expressions are computed. Since $s_1 = u_1(t)$, the remaining portion of investment resources allocated to the production and consumer subsystems is equal to $1 - s_1$. Let $l(t)$ denote the share of the consumer subsystem in this remainder of investment resources. Then, in order to ensure the fulfillment of the investment balance condition (4), the following allocation rule is applied:

$$s_1 = u_1(t), \;\; s_0 = l(t)(1 - s_1), \;\; s_2 = (1 - l(t))(1 - s_1). \tag{41}$$

To ensure the fulfillment of the labor balance condition (5), using the notations introduced in (12), we obtain the expressions for θ_0 and θ_2, while the expression for θ_1 is derived from (5) in the following form:

$$\theta_1 = \frac{1}{1 + \frac{s_0}{u_0(t)} + \frac{s_2}{u_2(t)}}, \;\; \theta_2 = \frac{s_2\theta_1}{u_2(t)}, \;\; \theta_0(t) = \frac{s_0\theta_1}{u_0(t)}. \tag{42}$$

Next, taking into account Equation (9) and the obtained values of θ_0 and θ_2 from Equation (46), the material balance Equation (6) yields the following expression for $l(t)$:

$$l(t) = \frac{\left(\beta_1 + \frac{h_1}{h_0}\gamma_1\right) A_1 y_1(t)^{\alpha_1} + \left(\beta_2 + \frac{h_2}{h_0}\gamma_2\right) A_2 \frac{(1-u_1(t))}{u_2(t)} y_2(t)^{\alpha_2}}{(1-\beta_0) A_0 \frac{(1-u_1(t))}{u_0(t)} y_0(t)^{\alpha_0} + \left(\beta_2 + \frac{h_2}{h_0}\gamma_2\right) A_2 \frac{(1-u_1(t))}{u_2(t)} y_2(t)^{\alpha_2}}. \tag{43}$$

2.5. Two-Pass Riccati–Adjoint Integration Procedure

The obtained optimality system consists of coupled matrix and vector differential equations. The coupling is resolved through a backward–forward integration procedure that avoids boundary-value shooting iterations (Algorithm 1).

https://doi.org/10.3390/computers15030179

First, the matrix equations are integrated backward in time, after which the state–adjoint system is integrated forward using the precomputed matrix functions.

Algorithm 1. Computational procedure for obtaining the optimal trajectory and control

Input: system matrices, parameters, y_0
Output: optimal trajectory $y(t)$, control $u(t)$

1. Set terminal condition $K(T) = F$.
2. Backward integrate Riccati-type equation for K.
3. Backward integrate transition matrix equation for $W(t, T)$.
4. Compute initial adjoint: $q(t_0) = W^{-1}(t_0, T)\ (y_0 - y_s)$.
5. For each time step $t \in [T, t_0]$:
   - Evaluate $K, W(t, T)$
   - Compute $\omega(y, t)$
   - Apply projection to obtain $u_i(t) = \min\{\rho_2, \max\{\rho_1, \omega_i(y, t)\}\}$
   - Update $\varphi(y, t)$
   - Integrate $(y(t), q(t))$ one step forward
6. Reconstruct balance variables:
   - To enforce the material balance constraint, expression (43) is evaluated
   - To enforce the investment balance constraint, expression (41) is evaluated
   - To enforce the labor balance constraint, expression (42) is evaluated
7. Return $y(t), u(t)$.

The algorithm does not involve outer fixed-point iterations or boundary-value shooting adjustments. The coupling between the matrix and vector equations is resolved sequentially through a single backward–forward sweep.

3. Computational and Structural Positioning

Consider the linear system

$$\dot{y}(t) = Ay(t) + Bu(t), \;\; y(t_0) = y_0, \;\; y(T) = 0, \tag{44}$$

with the following quadratic performance functional:

$$J(y, u) = \frac{1}{2}\int_{t_0}^{T} \Big(y^T(t)Qy(t) + u^T(t)Ru(t)\Big)dt, \tag{45}$$

The optimal control is given by the classical Riccati feedback as

$$u(t) = -R^{-1}B^T(Ky(t) + q(t)), \tag{46}$$

where K satisfies the differential Riccati equation, and the vector $q(t)$ arises due to the fixed terminal condition.

In the proposed formulation, the system dynamics have the structure (14), the cost functional includes the weighted control term $\big(D(y)u - D_s u_s\big)^T R \big(D(y)u - D_s u_s\big)$, and the control law takes the form (27). If we assume

$$D(y) \equiv I, \;\; \varphi(y, t) = 0, \;\; y_s = 0, \;\; D_s u_s = 0,$$

the nonlinear formulation reduces exactly to (44) and (46), which coincides with the classical finite-horizon LQR problem. Thus, the algorithm extends the classical Riccati framework to a class of nonlinear multi-module systems with state-dependent input operators and bilateral control constraints.

To provide a clearer methodological comparison, Table 1 summarizes the key computational and structural distinctions between representative optimal control frameworks.

Table 1. Comparison of the proposed algorithm with traditional optimal control methods.

Method	Single Shooting	Direct Collocation/ Transcription	Finite-Horizon LQR	MPC	RL/Neural Operators	Proposed Algorithm
Iterative boundary-value solution	Yes	No	No	Yes	No	No
Reformulates problem as large-scale NLP	No	Yes	No	Yes	No	No
Handles state-dependent input operator	Limited	Yes	No	Yes	Yes	Yes
Explicit bilateral constraints	Switching rules	As inequality constraints in NLP	No	Yes	Implicit	Analytically embedded
Analytical feedback structure	Yes	No	Yes	Receding-horizon	Approximate	Yes
Main computational structure	Forward–backward iteration	Nonlinear programming	Riccati ODE	Repeated online optimization	Offline training + inference	Two-pass Riccati–adjoint integration

4. Results

4.1. Numerical Experiments

To obtain a numerical solution to the formulated optimal control problem, a series of computational experiments were carried out using the proposed algorithm. Numerical simulations were performed over a finite planning horizon $T = 20$. The model parameters used in the computational experiments are presented in Table 2. The coefficients α_i, β_i, τ_i, and A_i were estimated on the basis of official statistical data of the Republic of Kazakhstan for the period 2010–2022 and reflect the structural characteristics of production, investment, and labor [24].

Table 2. Model coefficients.

i	α_i	β_i	τ_i	A_i
0	0.65	0.4	0.07	1.92
1	0.7	0.11	0.08	1.3
2	0.68	0.22	0.05	2.17

To construct the calculated trajectories and analyze the stability, the stationary values of the state and control variables presented in Table 3 were used. These stationary points were previously obtained using the methodology presented in [5] and are employed in the present study as reference equilibrium values.

Table 3. Stationary state of the nonlinear multi-module dynamic system.

i	θ_i	s_i	k_i	x_i	y_i
0	0.521	0.471	1390.574	110.485	33.624
1	0.325	0.37	1526.937	71.716	35.858
2	0.153	0.158	2227.593	62.781	31.390

https://doi.org/10.3390/computers15030179

The initial deviation of the system from the stationary state was specified in the following form:

$$y(t_0) = (-450,\ -300,\ -250)^*, \tag{47}$$

and the admissible control set was defined by bilateral constraints.

$$0.1 \le u_i \le 0.9,\ \ i = 0,\ 1,\ 2. \tag{48}$$

Figure 1 presents the time evolution of the deviations of the state variables $y_i(t) - y_i^s$ under optimal control.

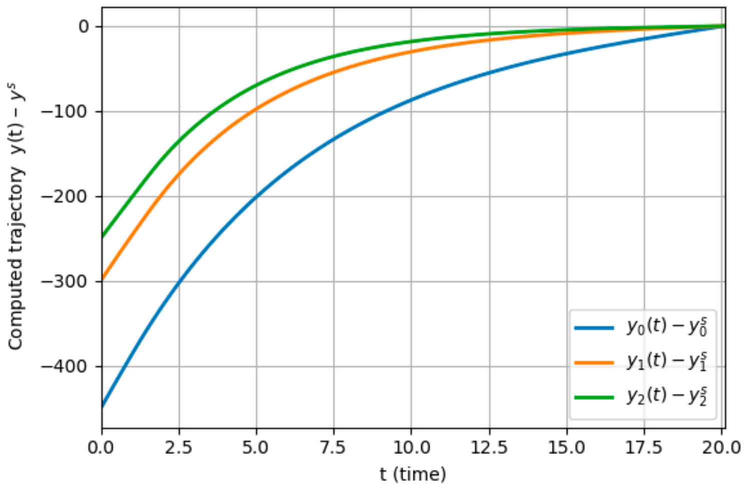

Figure 1. Dynamics of the state vector components $y_i(t) - y_i^s$ under optimal control for the three system modules.

As can be seen from the plots, all components of the state vector converged to their stationary values over the considered time interval. At the terminal time T, the deviations were

$$y_0(T) = 1.05 \times 10^{-4},\ \ y_1(T) = 2.31 \times 10^{-4}\ ,\ y_2(T) = -2.64 \times 10^{-4},$$

confirming the high numerical accuracy of convergence. The quantitative convergence characteristics of the computed trajectories are summarized in Table 4.

Table 4. Convergence metrics of the proposed optimal control algorithm.

Metric	Value
Initial deviation norm	595.819
Terminal deviation norm	3.661×10^{-4}
Relative reduction	6.144×10^{-4}
Settling time (1% criterion)	19.288

Figure 2 shows the computed trajectories of the optimal control. The obtained results demonstrate that the control inputs remain within the admissible set U over the entire time interval and strictly satisfy the bilateral constraints (48).

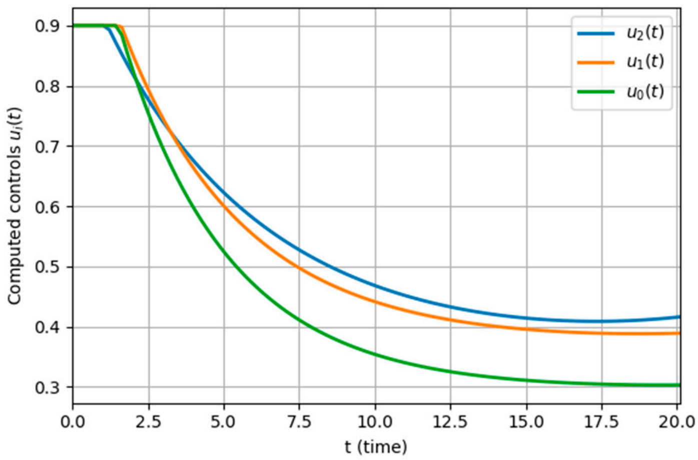

Figure 2. Dynamics of the computed optimal controls $u_i(t)$ satisfying the bilateral constraints.

Table 5 reports the numerical indicators related to the constraint enforcement and structural consistency of the model.

Table 5. Structural consistency and constraint satisfaction indicators.

Metric	Value
Integrated control energy	17.174
Lower bound activation	0.0%
Upper bound activation	8.0%

During the computational experiments, the optimal temporal distributions of labor resources θ_i and investment shares s_i among the production, investment, and consumer modules of the system were also obtained. The corresponding dynamics are presented in Figure 3.

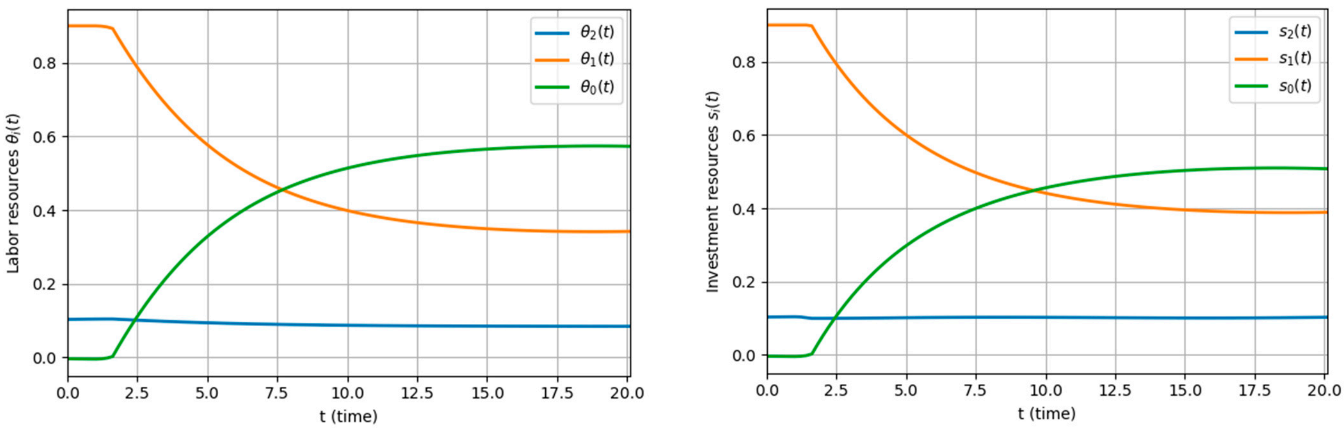

(**a**) (**b**)

Figure 3. Temporal dynamics of the optimal (**a**) labor resource distributions θ_i and (**b**) investment shares s_i.

Figure 4 shows the dynamics of the material balance relation (6).

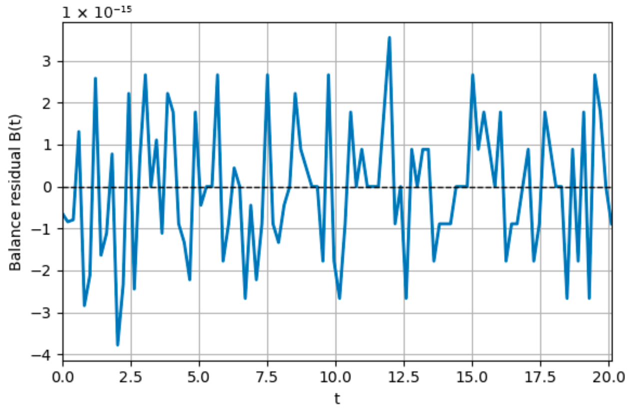

Figure 4. Dynamics of the material balance.

Over the entire time interval, the balance residual remains at the level of the numerical round-off error (approximately 10^{-15}), indicating the strict structural consistency of the computed solution. A quantitative summary of the balance preservation accuracy is presented in Table 6.

Table 6. Numerical accuracy of the material balance constraint.

Metric	Value
Max balance residual	3.774×10^{-15}
Mean balance residual	1.247×10^{-15}

Figure 5 presents the dynamics of the capital–labor intensity variables $k_i(t)$ and the normalized outputs $x_i(t)$. All variables exhibit stable behavior and converge to their stationary values.

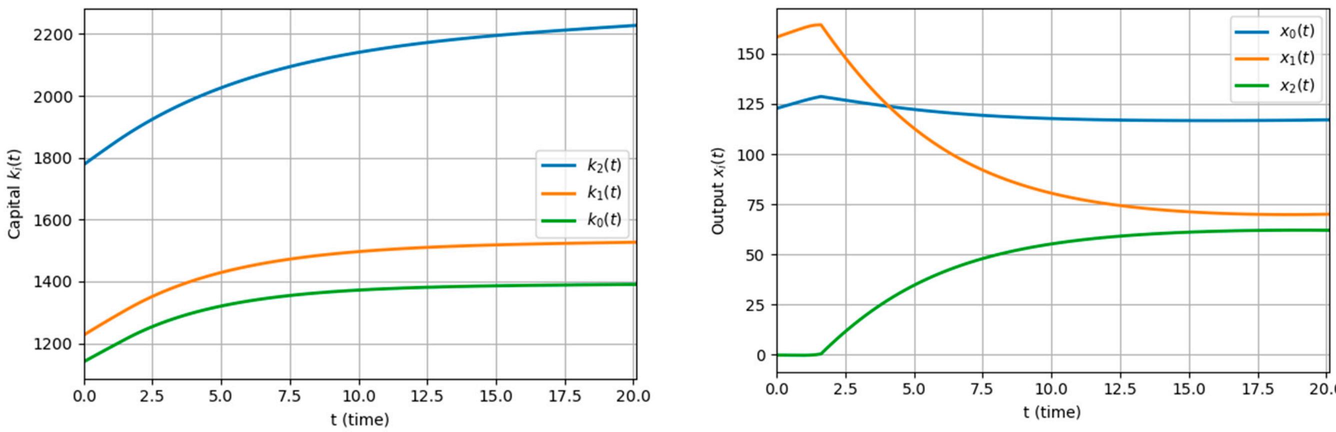

(**a**) (**b**)

Figure 5. Dynamics of the (**a**) capital–labor intensity variables $k_i(t)$ and the (**b**) normalized outputs x_i of the functional modules.

The computational scalability and solver sensitivity of the proposed algorithm are summarized in Table 7.

Table 7. Computational performance and numerical robustness analysis.

Metric	Result
Empirical complexity	$O(n^{3.182})$
State dimension $N = 40$ (CPU time)	0.320 s
State dimension $N = 80$ (CPU time)	6.296 s
State dimension $N = 100$ (CPU time)	19.764 s
Max deviation from reference $\left(\text{tol} = 10^{-6}\right)$	2.09×10^{-5}
Max deviation from reference $\left(\text{tol} = 10^{-7}\right)$	2.15×10^{-5}
Max deviation from reference $\left(\text{tol} = 10^{-8}\right)$	2.21×10^{-5}
RK45 (CPU time, $N = 40$)	0.0051 s
Radau (CPU time, $N = 40$)	0.308 s
BDF (CPU time, $N = 40$)	0.156 s
Inter-solver deviation	3.2×10^{-5}
Minimum eigenvalue of K	2.133×10^{-5}
Condition number of K	2.368

4.2. Parametric Analysis with Respect to the Coefficient γ_1

To assess the sensitivity of the optimal solution to the variations in external parameters, a parametric analysis was conducted based on the proposed optimal control algorithm, corresponding to the original mathematical formulation of the problem.

The parameter γ_1, which characterizes the maximum admissible share of imported investment goods, was varied, while keeping the remaining model parameters fixed.

Figure 6 demonstrates that an increase in the parameter γ_1 leads to a higher amplitude of the control inputs at the initial stage of the dynamics. Variations in γ_1 mainly influence the transient phase, while the terminal values remain nearly unchanged. For all considered parameter values, the trajectories $u_i(t)$ remain within the admissible bounds and retain a smooth behavior.

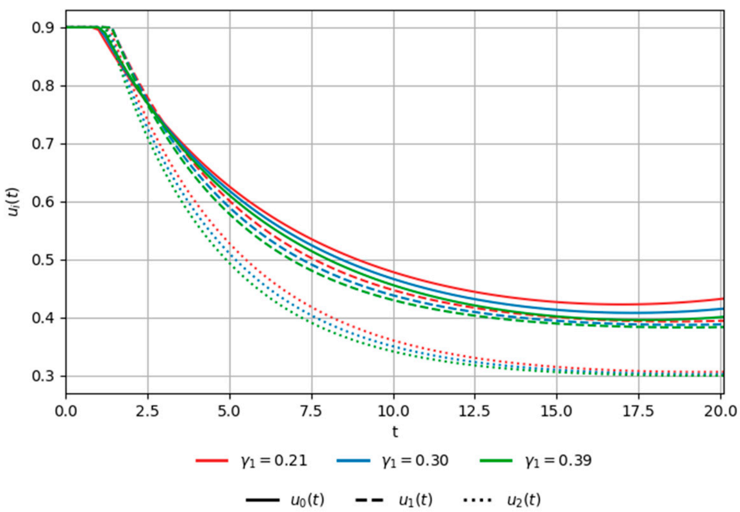

Figure 6. Dynamics of optimal control inputs $u_i(t)$ for different fixed values of γ_1.

Figure 7a,b present the corresponding dynamics of the labor resource distributions and investment shares.

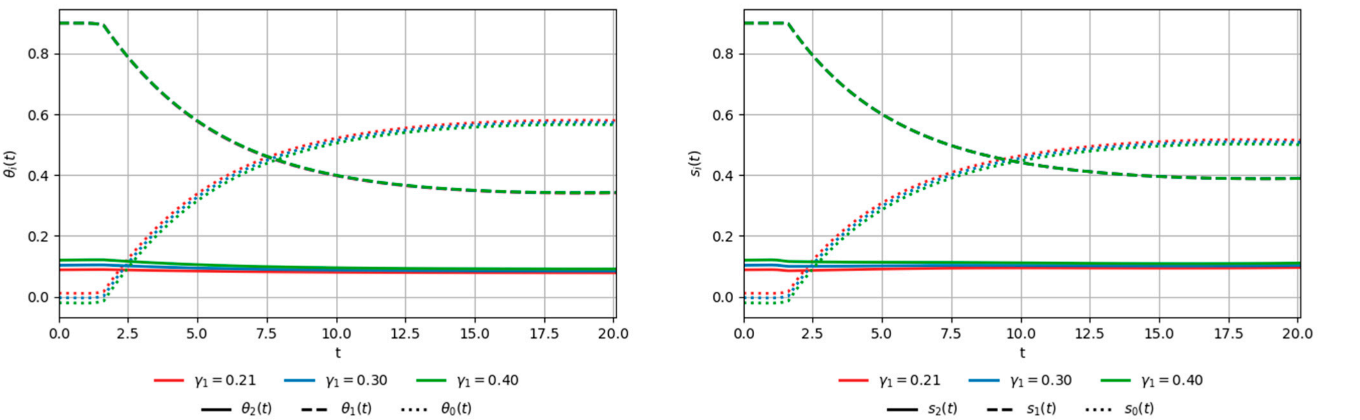

(**a**) (**b**)

Figure 7. Dynamics of resource allocation under variations in the parameter γ_1: (**a**) labor resource θ_i; (**b**) investment resource s_i.

An increase in the parameter γ_1 is accompanied by a decrease in the shares of labor and investment resources allocated to the production module (θ_0 and s_0) and their reallocation in favor of the investment module. A decrease in γ_1 produces the opposite structural effect: the shares θ_0 and s_0 increase, while the investment orientation of the system weakens. This behavior reflects the structural effect of importing investment goods: the higher availability of external investments reduces the need to support the domestic production module with internal resources and strengthens the system's orientation toward capital accumulation and expansion of its investment potential.

The dynamics of the material balance (Figure 8) show that, for all values of γ_1, the deviation of the balance relation remains on the order of 10^{-15} and oscillates around zero.

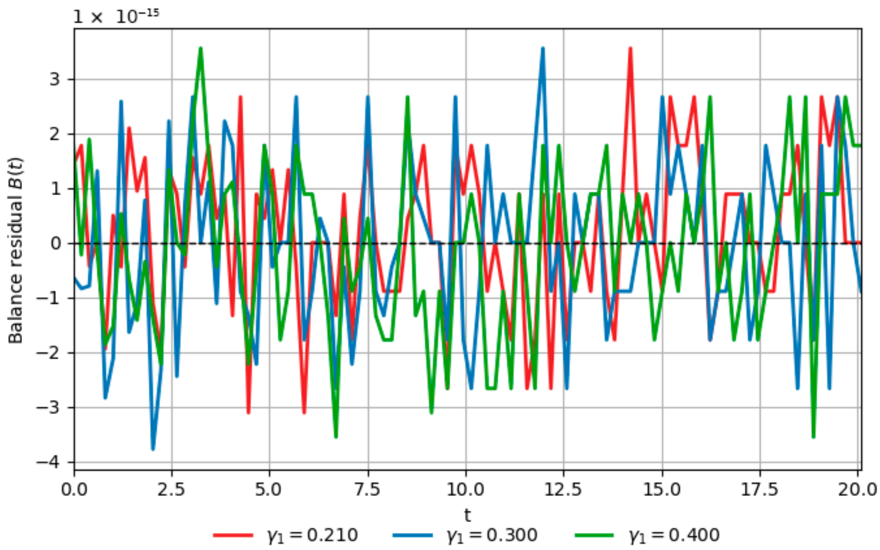

Figure 8. System balance under varying γ_1.

A quantitative summary of the influence of γ_1 on the convergence and control effort is presented in Table 8.

Table 8. Quantitative impact of the parameter γ_1 on the convergence and control performance.

γ_1	Terminal Deviation	Integrated Control Energy	Settling Time
0.21	3.34×10^{-4}	17.321	19.28
0.30	4.55×10^{-4}	16.830	19.28
0.39	3.85×10^{-4}	16.384	19.08

The results indicate that variations in γ_1 have only a minor effect on the terminal accuracy and settling time, while the integrated energy control slightly decreases as γ_1 increases.

4.3. Parametric Analysis with Respect to the Coefficient h_1/h_0

An additional parametric analysis was performed with respect to the coefficient h_1/h_0, which determines the relative ratio of the world prices of imported investment goods to exported resources.

Figure 9 indicates that variations in h_1/h_0 have only a minor impact on the control trajectories, reflecting their indirect dependence on the foreign trade balance.

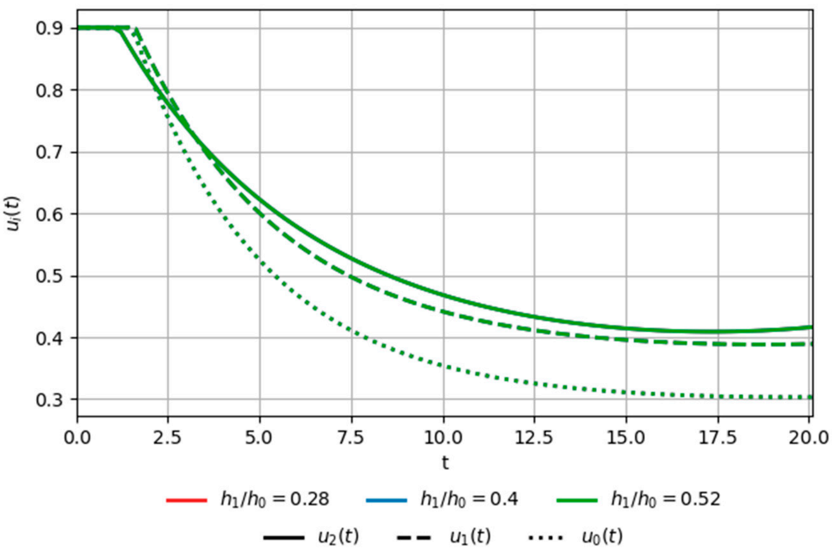

Figure 9. Control functions $u_i(t)$ for different h_1/h_0.

The same holds for the investment share s_1, since it is structurally defined by $s_1 = u_1(t)$. In contrast, the shares s_0 and s_2 exhibit noticeable redistribution as h_1/h_0 increases, reflecting adjustments in investment flows due to the higher relative costs of imported investment goods (Figure 10b).

Labor allocation exhibits stronger sensitivity: higher relative import prices increase employment in the consumer module and reduce labor in the investment module, while the production module remains largely unaffected (Figure 10a). This indicates structural rebalancing toward current output and domestic consumption under less favorable import conditions.

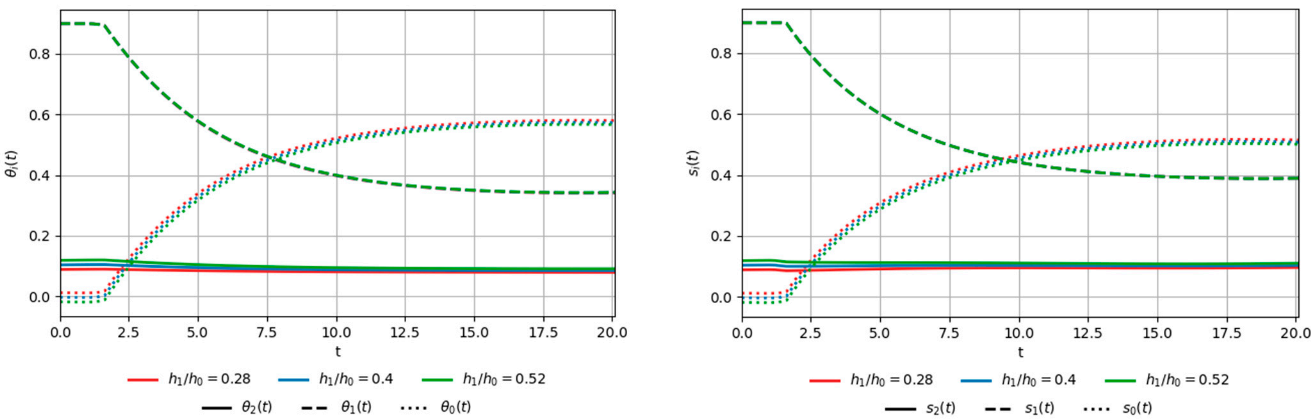

(**a**) (**b**)

Figure 10. Dynamics of resource allocation under variations in the parameter h_1/h_0: (**a**) labor resource θ_i; (**b**) investment resource s_i.

Figure 11 confirms preservation of the balance constraint for all parameter values.

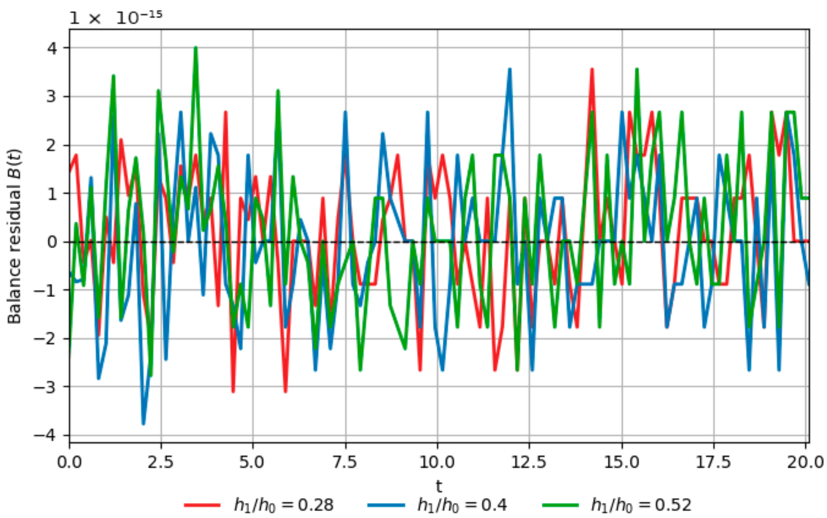

Figure 11. System balance under varying h_1/h_0.

Table 9 summarizes the quantitative sensitivity of the optimal solution to variations in the external price ratio. The results demonstrate a weak effect of h_1/h_0 on the terminal accuracy and control effort.

Table 9. Quantitative sensitivity of the optimal solution to variations in the price ratio h_1/h_0.

h_1/h_0	Terminal Deviation	Max Balance Residual
0.7	3.66×10^{-4}	3.44×10^{-15}
1.0	3.66×10^{-4}	3.77×10^{-15}
1.3	3.66×10^{-4}	5.33×10^{-15}

5. Discussion

The computational experiments confirm that the proposed optimal control algorithm generates admissible and structurally consistent state and control trajectories for the nonlinear multi-module system under bilateral constraints and balance relations. The state variables exhibit stable convergence over the finite planning horizon, with a monotonic reduction in the deviations and machine-level preservation of balance constraints.

The computed control inputs remain within the admissible set, and constraint activation occurs only locally without loss of smoothness. Resource redistribution during the transient phase compensates for the initial deviations, after which the system stabilizes near its stationary configuration.

The parametric analysis shows that the coefficient γ_1 regulates the trade-off between current production and investment-driven development, leading to the structural reallocation of labor and investment resources. In contrast, variations in the price ratio h_1/h_0 produce limited influence on the terminal accuracy and control effort, indicating the robustness of the optimal solution with respect to external price disturbances.

The model is formulated under deterministic assumptions with fixed structural parameters. Further research may incorporate stochastic effects and adaptive parameter identification to extend the applicability of the proposed framework.

6. Conclusions

In this study, we considered an optimal control problem for a nonlinear multi-module dynamic system under bilateral control constraints and external balance relations. A computational scheme based on a modified variational formulation was developed, allowing admissible controls to be generated within a unified dynamic framework without resorting to boundary-value shooting procedures or large-scale nonlinear programming.

The numerical experiments demonstrated stable convergence of the state trajectories, preservation of the structural balance constraints, and admissibility of the computed control inputs over the planning horizon. The parametric analysis illustrated how variations in key external coefficients influence the redistribution of investment and labor resources while maintaining numerical stability.

The proposed framework may be used as a computational tool for modeling and analyzing resource allocation processes in nonlinear dynamic systems. Further research may consider incorporating data-driven components, including machine learning techniques, for adaptive parameter estimation, improved forecasting of external disturbances, and acceleration of numerical procedures within the proposed control algorithm.

Author Contributions: Conceptualization, K.T.; methodology, K.T.; software, D.R. and Z.D.; validation, K.T., G.M. and D.R.; formal analysis, K.T.; investigation, K.T.; resources, K.T.; data curation, G.M.; writing—original draft preparation, K.T.; writing—review and editing, K.T. and G.M.; visualization, D.R. and Z.D.; supervision, K.T.; project administration, K.T.; funding acquisition, K.T. All authors have read and agreed to the published version of the manuscript.

Funding: This research is funded by the Science Committee of the Ministry of Science and Higher Education of the Republic of Kazakhstan (grant no. AP22684879).

Data Availability Statement: The raw data supporting the conclusions of this article will be made available by the authors on request.

Conflicts of Interest: The authors declare no conflicts of interest.

References

1. Montoya, O.D.; Serra, F.M.; Molina-Cabrera, A. Hierarchical Control for DC Microgrids Using an Exact Feedback Controller with Integral Action. *Computers* **2022**, *11*, 22. [CrossRef]
2. Murzabekov, Z.; Milosz, M.; Tussupova, K.; Mirzakhmedova, G. Development of an Algorithm for Solving the Problem of Optimal Control on a Finite Interval for a Nonlinear System of a Three-Sector Economic Cluster. *East.-Eur. J. Enterp. Technol.* **2022**, *1*, 43–52. [CrossRef]

3. Murzabekov, Z.; Milosz, M.; Tussupova, K.; Mirzakhmedova, G. Problems of Optimal Control for a Class of Linear and Nonlinear Systems of the Economic Model of a Cluster. *Vietnam J. Comput. Sci.* **2020**, *7*, 109–127. [CrossRef]
4. Ullah, I.; Lim, H.-K.; Seok, Y.-J.; Han, Y.-H. Optimizing Task Offloading and Resource Allocation in Edge-Cloud Networks: A DRL Approach. *J. Cloud Comput.* **2023**, *12*, 112. [CrossRef]
5. Tussupova, K.; Murzabekov, Z. Optimal Allocation of Resources in an Open Economic System with Cobb–Douglas Production and Trade Balances. *Economies* **2025**, *13*, 184. [CrossRef]
6. Kalamian, N.; Soltani, M.; Bouzari Liavoli, F.; Faraji Niri, M. Observer-Based Suboptimal Controller Design for Permanent Magnet Synchronous Motors: State-Dependent Riccati Equation Controller and Impulsive Observer Approaches. *Computers* **2024**, *13*, 142. [CrossRef]
7. Wu, X.; Zhang, K.; Cheng, M. Computational Method for Optimal Control of Switched Systems with Input and State Constraints. *Nonlinear Anal. Hybrid Syst.* **2017**, *26*, 1–18. [CrossRef]
8. Ganguly, S.; Randad, N.; D'Silva, R.A.; Raj, S.M.; Chatterjee, D. QuITO: Numerical Software for Constrained Nonlinear Optimal Control Problems. *SoftwareX* **2023**, *24*, 101557. [CrossRef]
9. Pappalardo, C.M.; Guida, D. On the Computational Methods for Solving the Differential-Algebraic Equations of Motion of Multibody Systems. *Machines* **2018**, *6*, 20. [CrossRef]
10. Drąg, P. A Direct Optimization Algorithm for Problems with Differential-Algebraic Constraints: Application to Heat and Mass Transfer. *Appl. Sci.* **2020**, *10*, 9027. [CrossRef]
11. Biral, F.; Bertolazzi, E.; Bosetti, P. Notes on Numerical Methods for Solving Optimal Control Problems. *IEEJ J. Ind. Appl.* **2016**, *5*, 154–166. [CrossRef]
12. Dapatadu, R.; Gibson, C.; Gregory, J. Numerical Methods for Nonlinear Optimal Control Problems: Application to Abnormal Problems. *J. Math. Anal. Appl.* **1991**, *159*, 27–43. [CrossRef]
13. Murzabekov, Z.; Miłosz, M.; Tussupova, K. The Optimal Control Problem with Fixed-End Trajectories for a Three-Sector Economic Model of a Cluster. In *Intelligent Information and Database Systems*; Nguyen, N.T., Hoang, D.H., Hong, T.-P., Pham, H., Trawiński, B., Eds.; Lecture Notes in Computer Science; Springer International Publishing: Cham, Switzerland, 2018; Volume 10751, pp. 382–391. ISBN 978-3-319-75416-1.
14. Trélat, E. Optimal Control and Applications to Aerospace: Some Results and Challenges. *J. Optim. Theory Appl.* **2012**, *154*, 713–758. [CrossRef]
15. Shiban, E.; Meyer, B. Treatment for Acute, Subacute and Chronic Low Back Pain. In *Spine Surgery*; Meyer, B., Rauschmann, M., Eds.; Springer International Publishing: Cham, Switzerland, 2019; pp. 3–8. ISBN 978-3-319-98874-0.
16. Benson, D.A.; Huntington, G.T.; Thorvaldsen, T.P.; Rao, A.V. Direct Trajectory Optimization and Costate Estimation via an Orthogonal Collocation Method. *J. Guid. Control Dyn.* **2006**, *29*, 1435–1440. [CrossRef]
17. Gornov, A.; Zarodnyuk, T.; Anikin, A.; Sorokovikov, P.; Tyatyushkin, A. Software Engineering for Optimal Control Problems. In *Mathematics and Its Applications in New Computer Systems*; Tchernykh, A., Alikhanov, A., Babenko, M., Samoylenko, I., Eds.; Lecture Notes in Networks and Systems; Springer International Publishing: Cham, Switzerland, 2022; Volume 424, pp. 415–426. ISBN 978-3-030-97019-2.
18. Patterson, M.A.; Rao, A.V. GPOPS-II: A MATLAB Software for Solving Multiple-Phase Optimal Control Problems Using Hp-Adaptive Gaussian Quadrature Collocation Methods and Sparse Nonlinear Programming. *ACM Trans. Math. Softw.* **2014**, *41*, 1–37. [CrossRef]
19. Grüne, L.; Pannek, J. *Nonlinear Model Predictive Control*; Communications and Control Engineering; Springer International Publishing: Cham, Switzerland, 2017; ISBN 978-3-319-46023-9.
20. Peng, Z.; Hu, J.; Shi, K.; Luo, R.; Huang, R.; Ghosh, B.K.; Huang, J. A Novel Optimal Bipartite Consensus Control Scheme for Unknown Multi-Agent Systems via Model-Free Reinforcement Learning. *Appl. Math. Comput.* **2020**, *369*, 124821. [CrossRef]
21. Recht, B. A Tour of Reinforcement Learning: The View from Continuous Control. *Annu. Rev. Control Robot. Auton. Syst.* **2019**, *2*, 253–279. [CrossRef]
22. Sakovich, N.; Aksenov, D.; Pleshakova, E.; Gataullin, S. A Neural Operator Using Dynamic Mode Decomposition Analysis To Approximate Partial Differential Equations. *AIMS Math.* **2025**, *10*, 22432–22444. [CrossRef]
23. Kolemayev, V. Optimalnyy Sbalansirovannyy Rost Otkrytoy Trehsektornoy Ekonomiki. *Prikl. Ekon.* **2008**, *11*, 15–42.
24. Tussupova, K.; Mirzakhmedova, G. Information System for Planning the Effective Distribution of Investment and Labor Resources Between Sectors of the Economy. In Proceedings of the International conferences on Economics and Social Sciences, Almaty, Kazakhstan, 23 June 2024; pp. 111–115.